

Phase-Change Materials: the view from the liquid and the metallicity parameter

Shuai Wei^{1*}, Pierre Lucas², and C. Austen Angell^{3*}

¹I. Institute of Physics IA, RWTH Aachen University, 52074, Aachen, Germany

²Department of Materials Science and Engineering, University of Arizona, Tucson, AZ 85712, USA

³School of Molecular Sciences, Arizona State University, Tempe, AZ, 85287, USA

While fast-switching rewritable non-volatile memory units based on phase-change materials (PCMs) are already in production at major technology companies like Intel (16-64 GB chips available), an in-depth understanding of the physical factors that determine their success is still lacking. Recently we have argued for a liquid phase metal-to-semiconductor transition (M-SC), submerged not far below the melting point T_m , as essential. The M-SC is itself a consequence of atomic rearrangements that are involved in a fragile-to-strong viscosity transition that controls both the speed of crystallization and the stabilization of the semiconducting state. Here we review the past work, and then introduce a new parameter, the “metallicity”, (the inverse of the average Pauling electronegativity of a multicomponent alloy). When T_m -scaled temperatures of known M-SCs of group-IV,V,VI alloys are plotted against their metallicities, the curvilinear plot leads directly to the composition zone of all known PCMs and the temperature interval below T_m , where the transition should occur. The metallicity concept may provide guidance for tailoring PCMs.

Keywords: phase-change materials, metal-semiconductor transition, metallicity, fragile-strong transition, fragility, liquid-liquid transition

1. Introduction

1.1. *The switching behavior of phase-change materials and the relevance of the liquid states*

* Email: shuai.wei@physik.rwth-aachen.de (S.W.), austenangell@gmail.com (C.A.A)

For more than half a century, mixtures of elements in the non-metal section of the periodic table have been famous for their ability to form glasses from their liquid states, often of great stability, low acoustic losses, and high corrosion resistance. They have found many applications particularly in infrared optics (night vision etc) and semiconductor electronics¹. However, as the compositions tested increase in heavier elements (e.g. Se replaced by Te), the glass-forming ability diminishes, seemingly as the band gap decreases. Whereas As_2Se_3 is extremely difficult to crystallize on laboratory time scales, Bi_2Te_3 is metallic and difficult to vitrify even by sputtering. In between is As_2Te_3 , which is seen to undergo a semiconductor-to-metal transition during heating above its melting point T_m ².

In 1968 Ovshinsky³ discovered that he could use the ability of the Te-containing alloys to generate solid phases of greatly differing electronic conductivities depending on whether they were vitreous or crystalline, to make switching devices, and memory devices. Apart from some excellent fundamental studies in Ovshinsky's laboratory, however, developments were slow, with a resurgence of interest only in late 1980s after Yamada et al.⁴ published a study on the three-component system Ge-Sb-Te showing special behavior along what we will call the "Yamada line", (the composition line joining GeTe to Sb_2Te_3). The Yamada line⁵ features several closely related crystalline compounds of simple structure and remarkably fast crystallization kinetics. These crystalline compounds have been given detailed study by Wuttig, who in 2005 highlighted the storage potential of devices containing them⁶. A follow-up 2007 paper on the subject by Wuttig and Yamada in collaboration⁷, has been greatly cited. It is only very recently though, that this interest has been translated into manufactured devices, and even more recently that attention has been directed to the liquid states of PCMs to understand their special crystallization properties⁸⁻¹². In this contribution, we review these liquid state issues and then take the development one step further by introducing and exploiting a new material parameter, the "metallicity". Using this parameter in our plots allows us to strengthen the claim

that it is the existence of a M-SC submerged a critical distance below T_m that makes it possible for these new PCMs to perform as they do.

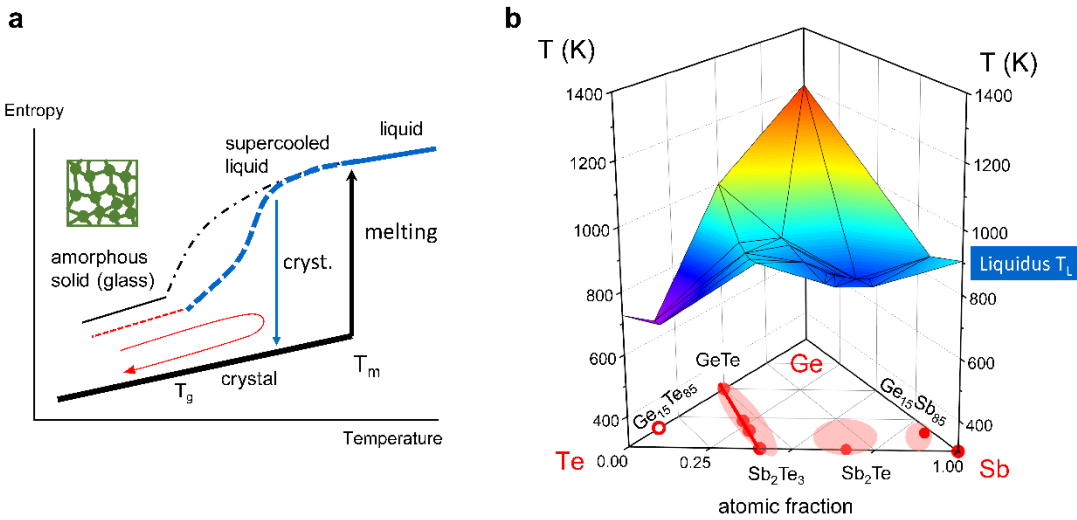


Figure 1. (a) A schematic plot for the entropy of a typical glass forming liquid (dot-dashed line) and a switchable phase-change material (dashed line) in an alternative scenario with additional entropy loss. (b) The liquidus surface¹³ (contour) of the ternary Ge-Sb-Te. The solid red dots and shadow areas indicate the common compositions of PCMs for memory and data storage applications⁷.

First we give a brief introduction to glass-forming liquid phenomenology. Figure 1 illustrates both paradoxical and practical aspects of the typical glassforming liquid, by which term we mean a liquid that is slow to crystallize on cooling below its T_m . The figure shows how the excess entropy of the liquid introduced on melting is decreasing rapidly as supercooling is extended, in consequence of the higher heat capacity of the liquid. It is evident that the entropy of the liquid would fall below that of the crystal far above 0 K were it not for the intercession of a structural arrest phenomenon called the “glass transition” (T_g) at which the heat capacity (C_p) contribution coming from configurational changes with temperature, drops out. The avoiding of a thermodynamic catastrophe by a

kinetic phenomenon is known as the Kauzmann paradox and has attracted much attention from the theoretical community.

On the other hand, in PCMs, which are poor glass formers, this scenario is only realized when the cooling rate is very high, meaning that the glassy state that is trapped would be high in entropy and low in stability relative to more slowly cooled structures if not assisted by some additional source of entropy loss that will be the focal point of this contribution.

The action of reheating the glass, by heat pulse, to a temperature kept well below T_m provides a new opportunity for the glass to crystallize, and then the crystal, with more ordered structure and much higher electronic conductivity, can generate the “on” state of a microscopic “bit” of the material. This is illustrated by the red heat-and-cool arrow in the figure. If the heat pulse is sufficient to raise the temperature *above* T_m , and the surroundings provide a good enough heat sink, then the cooling rate after the pulse will be sufficient to return the sample to the glassy, or “off”, state. In PCMs this fine-tuned and complex sequence can be repeated countless times with high reproducibility, allowing for fabrication of a chip with huge storage capacity¹⁴⁻¹⁶.

Figure 1b shows the relation of the liquidus surface of the system Ge-Sb-Te in relation to the composition of known PCMs¹³, in particular the Yamada line of crystals that has been given the most attention. The PCM compositions all have low T_m , but apparently not the lowest or PCMs would be concentrated at the ternary eutectic composition which is the most easily glass-forming.

1.2 No-man’s land of phase-change materials

The problem with identifying the additional source of entropy loss that was mentioned above is that it clearly must occur below the T_m and of course well above T_g . The fact that the crystallization rates of PCMs, in contrast to the chalcogenide glassformers of earlier studies, are extremely high, means that it is very difficult to characterize what the additional source of entropy loss might be by direct experiment. The problem is very reminiscent of that of supercooled

water, the “most anomalous liquid”, which has been the source of so much interest because of the apparent existence of a transition of higher order, (close to first order), lying about 20% below the T_m .

In the case of water, the thermodynamic properties which are so well known in the stable range between 0 and 100°C, develop striking anomalies as the liquid is supercooled. With samples of extreme cleanliness these can be studied down to the “homogeneous nucleation temperature” T_h near -31 °C for large (10ml ampoules) and -38°C for micron sized samples (special emulsions). The isothermal compressibility, for instance, increases according to a power law with an apparent divergence temperature of 228K, implying proximity to a critical point. So far, comparable supercoolings have not been reported for PCMs.

This cut-off on measurements near T_m , and a corresponding termination of the glassy state due to fast crystallization at far lower temperatures, establishes the existence of a “no-man’s land” (a term used for the water problem) in which no observations can be made except by ultrafast probes or deduction from external studies such as crystallization rates. In the next sections, we will make use of a simpler and more powerful approach using plausible extrapolations of the properties of many non-PCM, but related, materials, to reach the conclusions about the PCMs themselves. In this approach, we will be greatly aided by the metallicity parameter mentioned above.

2. Thermodynamic response functions in group-VI,V,VI liquid alloys

2.1 Density and thermal expansivity anomalies

Three elements and many group-IV,V,VI alloys exhibit temperatures of maximum density(T_{MD}) in their liquid states, an anomaly often mistakenly thought to be unique to water. In Figure 2, the available liquid densities are plotted against T_m -scaled temperature. The elements and alloys exhibiting a density maximum, include Te (direct measurement), Si and Ge (by computer simulation extension of experimental data), GeTe₁₂, GeTe₆ (i.e. Ge₁₅Te₈₅), In₂Te₃, As₂Se₃, As₂Te₃, and Ga₂Te₃ as well as In₂Te₃¹⁷ and Te_x-Se_{1-x}¹⁸ (not shown). The T_{MD} is ~0.9 T_m for tellurium. Liquid silicon undergoes a first-order LLT during

supercooling seen as a sharp density decrease at around $0.65T_m$ in computer simulations¹⁹. Most of observable density maxima are above T_m (i.e. $T_{MD} > T_m$). Those with compositions typical of PCMs such as GeTe, Sb₂Te₃, and Ge₁Sb₂Te₄, Ge₂Sb₂Te₅ on the Yamada line, do not display a density maximum above T_m ²⁰. But when we include the measured density of the glassy phase obtained by sputtering or hyperquenching and compare with the behavior of nearby compositions that do exhibit density maxima, it is highly plausible to interpolate density traces with maxima.

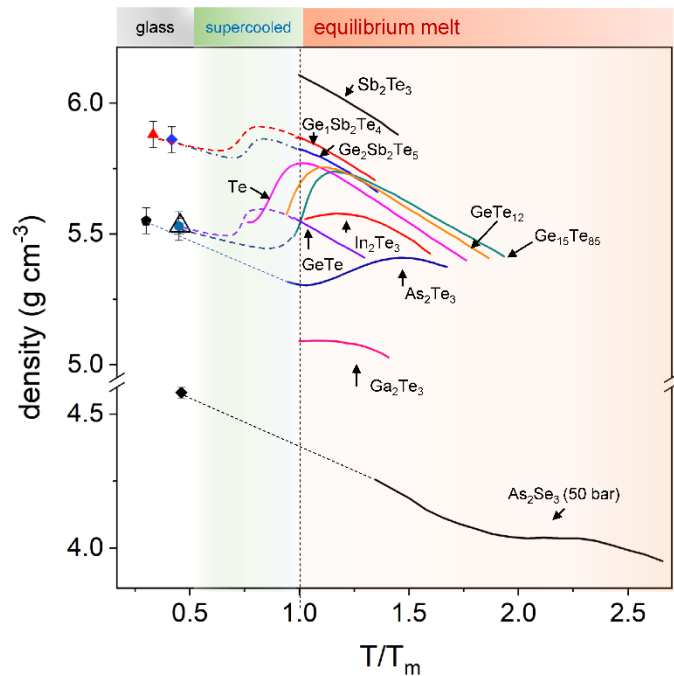


Figure 2. Liquid densities vs. T_m -scaled temperature. The low-temperature data points are for glassy states, and dashed lines are interpolations of the density traces in the supercooled liquid regime based on the evidence from the cases of As₂Te₃ (ref.²) and As₂Se₃ (ref.²¹) that the density follows a negative slope with respect to temperature below the T_{MD} . Data of GeTe, Sb₂Te₃, and Ge₁Sb₂Te₄, Ge₂Sb₂Te₅ are from ref.²⁰. The data for Te, GeTe₁₂, GeTe₆ (Ge₁₅Te₈₅) are from ref.²². For the glassy states, Ge₁Sb₂Te₄: $\rho = 5.88 \text{ g/cm}^3$, ref.²³, Ge₂Sb₂Te₅: $\rho = 5.88 \text{ g/cm}^3$, ref.²⁴, GeTe: $\rho = 5.6 \text{ g/cm}^3$ ref.²⁵, As₂Te₃: $\rho = 5.53 \text{ g/cm}^3$ ref.²⁶, and Ge₁₅Te₈₅: ρ of Ge₁₇Te₈₃ is available and assumed to be approximately the same 5.53 g/cm³ ref.²⁷.

Note that between the density maximum and the density minimum there lies an extremum in the thermal expansivity, $\alpha_p = V^{-1}(\delta V/\delta T)$, the temperature of which corresponds to the peak in the heat capacity (next section). It also corresponds closely with temperature of the closing of the band gap (see Figure 3 below), and other properties that relate to M-SC. It is obvious that the width of the $\alpha_p(T)$ peak will be correlated with the sharpness of $\rho(T)$ maximum.

2.2. Heat capacity anomalies

Where heat capacities have been measured for the systems shown in Figure 2, they show maxima that coincide with the maximum in α_p mentioned in the previous section. The width of the anomalies is also comparable. The sharpest C_p anomalies have been observed for elemental Te and the Ge₁₅Te₈₅ eutectic alloy, which have been correlated with the fragile-strong transition (FST) in the viscosity that will be discussed in a later section. These sharp anomalies lie at or below the thermodynamic T_m . Cases observable above T_m tend to be broader but of course are easier to study. The case of As₂Te₃ in particular has been characterized by not only C_p and density measurements but also Knight shift² and electronic conductivity data which are assembled in Figure 3.

3. Metal-semiconductor transition vs. metallicity in phase-change materials

The maxima in thermodynamic response functions are, in each case, accompanied by conductivity transitions in group-VI, V, VI alloys in which conductivities σ decrease from almost temperature-independent values slightly above $\sigma = 1000$ S cm⁻¹ (Mott's "minimum metallic conductivity"), to the lower and temperature-dependent values characteristic of semiconductors²⁸ (Figure 3c). The transition, designated M-SC, is also evident in the closing of the optical band gap E_g in As₂Se₃ liquid²⁹ (Figure 3b).

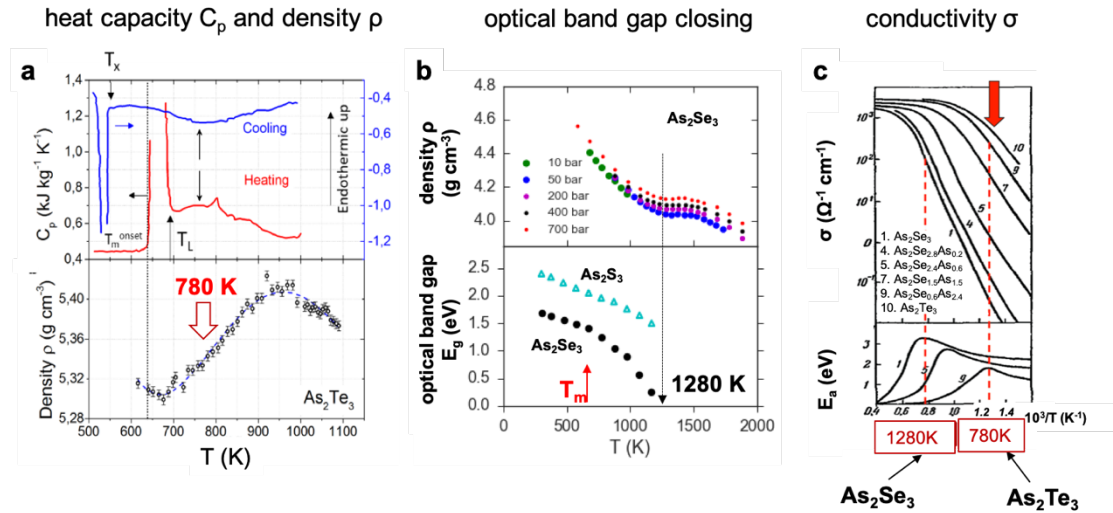


Figure 3. The metal-semiconductor transition. (a) The C_p maximum is ~ 80 K above the liquidus T_L in As_2Te_3 . Lower: the density maximum and minimum of liquid As_2Te_3 (ref.²). (b) Upper: Densities of liquid As_2Se_3 at various mild pressures. Lower: Optical band gap of liquid As_2Se_3 closes at ~ 1280 K, and that of As_2S_3 would close at a higher temperature^{21,29}. (c) Electronic conductivity σ for $(\text{As}_2\text{Se}_3)_{1-x}(\text{As}_2\text{Te}_3)_x$ alloys. The σ drops from a plateau of $\sim 10^3$ S cm⁻¹ through a M-SC. The T_{M-SC} corresponds to the maximum in apparent activation energy of σ (ref.^{28,30}).

Considering the series As_2S_3 , As_2Se_3 and As_2Te_3 , in Figure 3, it is clear that the M-SC transition moves to lower temperatures as the chalcogenide becomes more metallic, and the same is true for the series Sb_2S_3 , Sb_2Se_3 and Sb_2Te_3 (which latter actually melts to the metallic phase, see Fig. 3 of ref.¹¹). Finally, the trend holds for the binary solutions Se-Te (ref.³¹). In an attempt to quantify this trend we introduce a new parameter, the “metallicity”, which we

define as the inverse of the composition-averaged electronegativity of the alloy, according to

$$M_P = 1/(x_1 \cdot \chi_{P1} + x_2 \cdot \chi_{P2} + \dots + x_i \cdot \chi_{P3})$$

where $0 < x_i < 1$ is the atomic fraction of the alloy component i , and χ_{Pi} is available for each element in any Table of revised Pauling electronegativities³² (hence the subscript P).

In Figure 4a, we use this parameter to rationalize the variation of the temperature of the M-SCs when scaled by the alloy melting points (or liquidus for Te-Se)

$$t_{M-SC} = T_{M-SC}/T_m.$$

For low M_P chalcogenides like As_2Se_3 and $\text{Te}_{40}\text{Se}_{60}$, the t_{M-SC} is larger than 1.0. With increasing metallicity, t_{M-SC} decreases, approaching the value of 1.0 around $M_P = 0.47-0.48$. For any IV,V,VI alloy with $M_P > 0.48$, t_{M-SC} , the M-SC transition falls below T_m . While the correlation is clear for group-IV,V,VI alloys, the group-III,VI alloys (e.g. In-Te, green diamonds) are displaced, suggesting that a volume scaling might also be a needed addition.

For PCM compositions on the Yamada line e.g. $\text{Ge}_1\text{Sb}_2\text{Te}_4$ and $\text{Ge}_2\text{Sb}_2\text{Te}_5$, M_P lies between 0.481 and 0.487 (pink shadow area), and the Fig. 4 correlation line suggests their M-SCs, should all be “submerged” below T_m ($t_{M-SC} < 1.0$, as our earlier study suggested¹¹). Note that the PCM compositions $\text{Ge}_{15}\text{Sb}_{85}$ and (Ag, In-doped) Sb_2Te are *not* on the Yamada line, but they have similar values of M_P , viz = 0.48-0.49 in the same zone of metallicity³³.

In Figure 4b, the absolute values of T_{M-SC} are plotted against M_P , showing a V-shape, where all known PCM compositions are located in the minimum zone around $M_P=0.48-0.49$. This zone appears to be crucial for group-IV,V,VI PCMs, as it corresponds to a lowest T_{M-SC} , and meanwhile, ensures $t_{M-SC} < 1.0$. Their relevance to fast switching lies on a transition in kinetic properties at the same temperature T_{M-SC} , known as a fragile-strong transition (FST).

Following these successes, we have noted that the element bismuth Bi has nearly the same metallicity as Ge (0.495 and 0.498 respectively), hence might be predicted to replace Ge in PCM formulations. Indeed, we find that Bi_2Te_3 has been identified by atomic probe tomography as having the bonding of a PCM³⁴, and Bi_2Te_3 nanowires exhibit memory switching behavior³⁵. It raises the question “is there perhaps an equivalent of the “Yamada line” in the Bi-Sb-Te system (Ge-free), e.g. along much of the Bi_2Te_3 - Sb_2Te_3 join?” Both are in the weak metal state at their melting temperatures, like PCMs. Attention was already drawn to the analog of the GST Yamada line provided by the (Ge-containing) Ge-Bi-Te system³⁶ and to the similarity of the various crystalline structures along that line to those in the GST system. In that case it was reported that the presence of Bi “significantly enhances the crystallization of the GBT layers”.

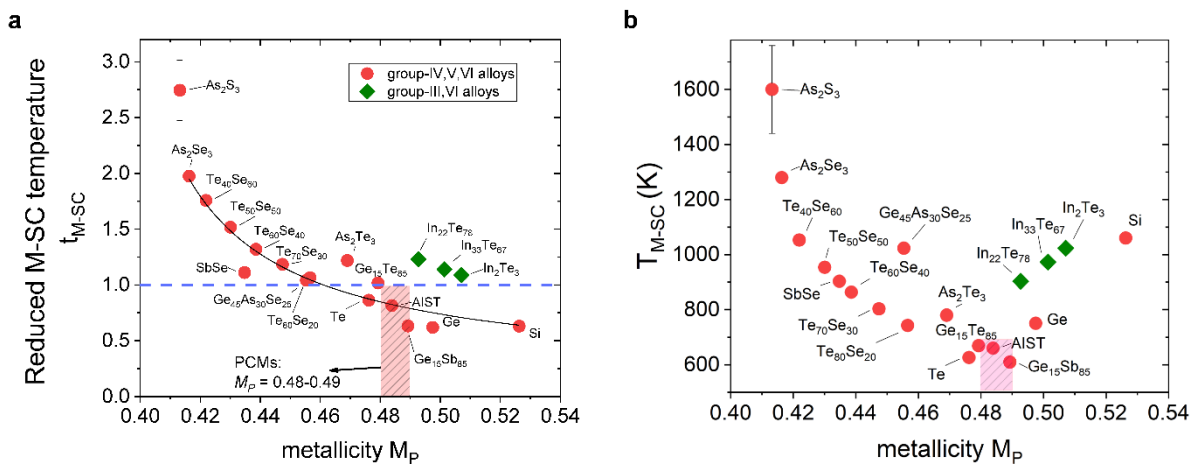


Figure. 4. Correlations of alloy T_{M-SC}/T_m , and T_{M-SC} values with the metallicity parameter, M_P . (a) The t_{M-SC} ($= T_{M-SC}/T_m$) of group-IV, V, VI alloys (red dots) and group-III, VI alloys (green diamonds). The PCM compositions on the Yamada line, and AIST and $\text{Ge}_{15}\text{Sb}_{85}$ have a metallicity ranging $M_P=0.48-0.49$, marked by the shadowed pink area, which corresponds to $t_{M-SC}<1.0$. (b) The absolute T_{M-SC} relation to metallicity M_P . This shows a V-shape with respect to M_P with a minimum zone (shadowed pink zone), where all known PCMs are

located. Data sources: As_2Se_3 and As_2S_3 : ref.²⁹; $T_{\text{M-SC}}$ of As_2S_3 is an extrapolation to optical band gap closing; Te-Se: ref.³¹, SbSe: ref.³⁷, $\text{Ge}_{45}\text{As}_{30}\text{Se}_{25}$: ref.³⁸; The $T_{\text{M-SC}}$ is assigned to the temperature of maximum slope of density curve ~ 750 °C = 1023 K. As_2Te_3 : ref.², Te: ref.²², $\text{Ge}_{15}\text{Te}_{85}$: ref.^{10,22}, In-Te: ref.¹⁷, Ge: ref.³⁹, Si: ref.¹⁹, AIST and $\text{Ge}_{15}\text{Sb}_{85}$: ref.³³.

4. Double-kink and smeared-out fragile-strong transitions in viscosity

In the classic 1965 paper of Adam and Gibbs⁴⁰, the authors presented a molecular kinetic theory in which the temperature dependence of relaxation time $\tau(T)$ is determined by the probability of cooperative rearrangement of mobile units in the system. The latter can be expressed in terms of configurational entropy, S_c .

$$\tau = \tau_0 \exp[-C/(TS_c)]$$

where τ_0 is the pre-exponent near the phonon cycle time (10^{-14} s). In treating experimental data, S_c has been shown to be proportional to the excess entropy S_{ex} of liquid over crystal, which can be derived from C_p ¹⁰. Thus, the C_p maximum leads to a transition in $\tau(T)$ and therefore the viscosity $\eta(T)$ (through the Maxwell relation $\eta = G_\infty \cdot \tau$), i.e. a FST.

A clear FST is demonstrated in $\text{Ge}_{15}\text{Te}_{85}$ (Figure 5) as a ‘double-kink’ in $\eta(T)$ -curve near its eutectic temperature, which is verified by a direct DSC measurement near T_g ¹⁰. The corresponding structural change is shown as a stepwise rise in r_2/r_1 of reduced pair distribution functions $G(r)$ from in-situ X-ray scattering⁴¹. In As_2Te_3 , the FST is so smeared-out that no ‘double-kink’ is discerned. The C_p anomaly spans ~ 300 K (Figure 3a). The viscosity of As_2Te_3 drops smoothly by ~ 3 orders of magnitude in the transition range. The sharpness of the FST depends on the sharpness of the C_p maximum and the associated loss of S_{ex} across the transition. (A first order transition must be accompanied by a stepwise viscosity increase, and in many cases would take the system directly into the glassy state).

The viscosity of PCM compositions has been measured directly for $\text{Ge}_2\text{Sb}_2\text{Te}_5$, (Ag, In)-doped Sb_2Te (AIST), GeTe etc. at high temperatures above their T_m , as shown in Figure 5. Those data nearly overlap the high-temperature viscosity of Te (orange triangles) and that of the fragile state of $\text{Ge}_{15}\text{Te}_{85}$ above its

FST (open circles) at $T_g/T < 0.5$. Thus, liquid PCMs above T_m exhibit a “fragile” behavior, as expected from their weak-metal states in the equilibrium melt.

Insofar as the predicted FSTs (hence also M-SCs) always occur below T_m in PCMs, they cannot be directly observed due to the interference of fast crystallization, but have only been inferred. For as-deposited AIST, Orava et al.^{42,43}, measuring the T-dependence of crystallization kinetics using ultrafast DSC, and inferred an ‘Arrhenius’ like behavior of viscosity between 383 K and ~490 K. They proposed a broad crossover from a high-temperature fragile liquid ($m = 74$) to a low-temperature strong liquid ($m = 37$). Zalden et al.⁴⁴ identified a crossover temperature in AIST (~570 K for melt-quenched samples and ~540 K for as-deposited samples) through the kinetics of sub-nanosecond laser induced crystallization. In the same composition, Salinga et al.⁴⁵ revealed a nearly constant activation energy for the T-dependence of crystal-growth-derived viscosity below ~570 K, which they referred to as Arrhenius-like behavior. This was attributed to the falling out of equilibrium into glassy states due to extremely fast cooling rates ($\sim 10^9$ - 10^{10} K/s) by laser-melt-quench on the small beam spot. The *ab initio* calculation of Zhang et al. for AIST⁴⁶ has successfully produced reasonable T-dependence of diffusivity at high temperature above T_m , though did not give a reasonable account for the supercooled liquid state at much lower temperatures. For $\text{Ge}_2\text{Sb}_2\text{Te}_5$, the ultrafast DSC study of Orava et al.⁸ implies a single fragility parameter ($m \approx 90$) for the entire liquid regime, while the *ab initio* simulation of Flores-Ruiz and Micoulaut⁴⁷ proposed a FST from $m \geq 129$ to $m=90$ at 792 K. The ultrafast DSC study of $\text{Ge}_2\text{Sb}_2\text{Te}_5$ nanoparticles suggested a broad FST. In another PCM GeTe, a single fragility ($m = 76$) is suggested, partially based on ultrafast DSC measurements, to describe the liquid without a FST⁴⁸, which is in contrast to the extrapolation from ref.¹¹ and this work. Zhang et al.¹⁶ emphasized a “kinetic crossover”, defined as a large change in activation energy of viscosity, that occurs somewhat below T_m , as essential for fast crystal growth in PCMs. Note that a so-defined “kinetic crossover” is not the same concept as the FST discussed here (or fragile-strong crossover), because the former is expected during the undercooling of any fragile liquid that is described by mode coupling theory (MCT)⁴⁹ at higher temperatures. It corresponds to the much-discussed crossover from MCT to “hopping” behavior, i.e. it does not imply a structural or heat capacity-based transition to a stronger liquid state.

Unlike the cases of good glass-formers (e.g. $\text{Ge}_{15}\text{Te}_{85}$ and As_2Te_3), the ambiguity and controversy of fragilities and FSTs in PCM compositions are no surprise because no direct experiments can be carried out in the fast crystallization regime to determine the viscosity of supercooled liquid. In the literature, the reported crystal growth velocities themselves may differ by a few orders of magnitude, depending on different sample preparation processes and experimental approaches. Furthermore, since crystallization processes may occur in either glass or liquid, and since the glass transition temperatures of PCMs are still debated, it is unclear whether the derived viscosity corresponds to the *equilibrium* viscosity that is the meaningful quantity for discussion of liquid fragility, or something else. For instance, if a liquid falls out of equilibrium during cooling and forms a glass at a fictive temperature T_f , which depends on the cooling rate, a quantity with dimensions of viscosity can still be measured, and it usually follows the Arrhenius law⁵⁰, but this behavior should not be confused with that of a strong liquid, nor the transition to the strong state, a FST.

It is only very recently that a femtosecond pump-probe x-ray laser experiment of Zalden et al³³, that enables resolution of structural changes within nanosecond timescales, has provided the first direct evidence of a structural transition in PCMs below T_m . This was observed at 660 K in AIST ($\text{Ag}_4\text{In}_3\text{Sb}_{67}\text{Te}_{26}$) and 610 K in $\text{Ge}_{15}\text{Sb}_{85}$, and is so far the most convincing evidence of LLTs (simultaneous M-SCs) in the supercooled liquid PCMs. When the results are plotted in Fig. 4, the data well support our prediction from the metallicity parameter.

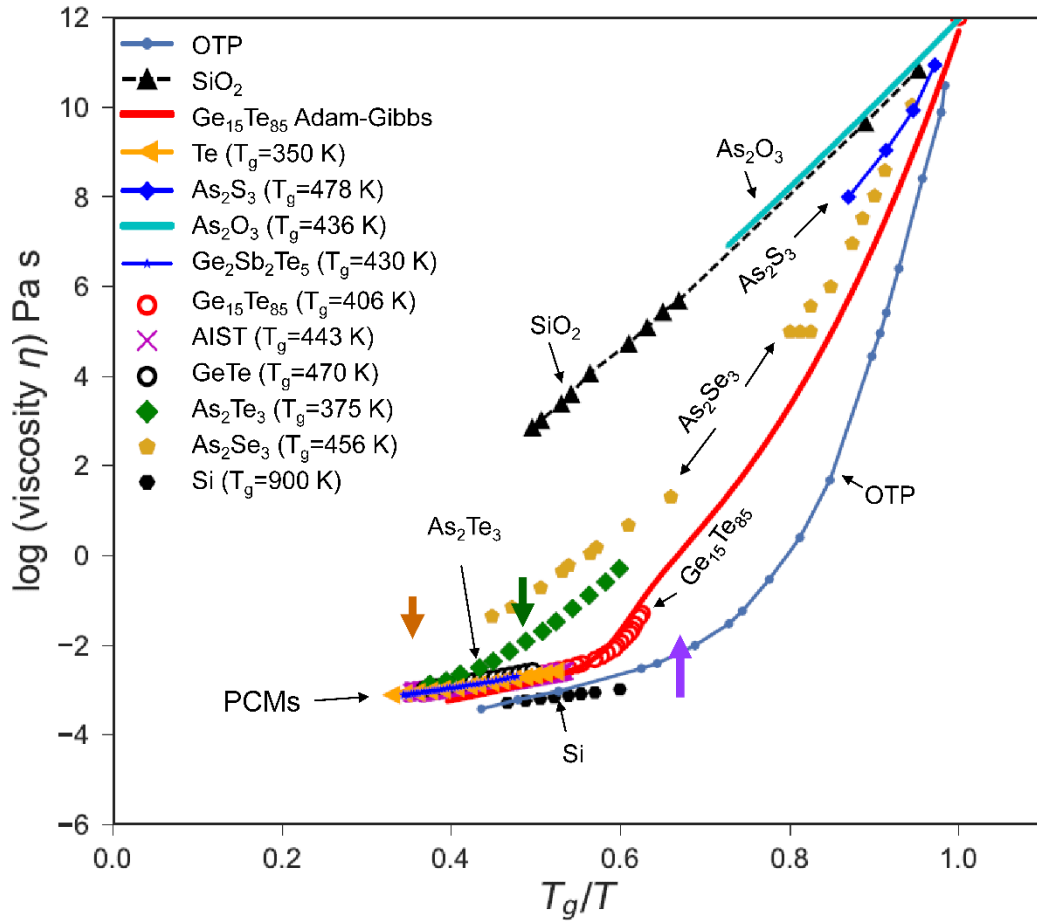


Figure 5. T_g -scaled Arrhenius plot for viscosity η of group-IV, V, VI alloys.

PCMs, which have the highest metallicity, exhibit the lowest viscosities at T_m (where $T_g/T_m \sim 0.5$). On the reduced T_g -reduced scale they overlap the elemental Te data). Alloys of lower metallicity exhibit systematically higher viscosities, and lower m fragilities. The lowest metallicity case, As_2O_3 , with $m = 19$ (according to light scattering relaxation time data) is even stronger than the archetypal strong liquid, SiO_2 . Apart from this interesting case, Figure 5, contains only directly measured experimental viscosities. The crystal-growth-derived viscosities are not shown. The bold colored arrows indicate $T_{\text{M-SC}}$ of AlST (purple) below T_m , and that of As_2Te_3 (green), and As_2Se_3 (orange) above T_m , respectively. Data sources: $\text{Ge}_2\text{Sb}_2\text{Te}_5$: ref.⁵¹; $T_g = 430$ K is taken from ref.⁵², although the value is still under debate⁸. AlST (Ag-In-doped Sb_2Te): ref.⁴²; its $T_g = 443$ K ref.⁵² is also under debate⁴³. Te: ref.⁵³; $T_g = 350$ K is estimated by ref.¹¹. $\text{Ge}_{15}\text{Te}_{85}$: viscosity data⁵⁴; Adam-Gibbs fitting line¹⁰. GeTe: ref.⁴⁸ assigned $T_g = 470$ K. As_2Te_3 : ref.⁵⁵. $T_g = 375$ K is the value at which calculated

viscosity reaches 10^{12} Pa s. As_2Se_3 : ref.⁵⁶; As_2S_3 : ref.⁵⁷. For As_2O_3 , relaxation times were directly measured using light scattering, from which the precise VFT parameters were obtained. The viscosity is represented by a VFT fit in the similar temperature range of relaxation time data using the parameters in ref.⁵⁸; SiO_2 , and OTP: ref.⁵⁷. Si: ref.⁵⁹. The T_g of Si is unknown and here assigned as 900 K¹⁰.

We further comment on the significance of FSTs due to the sharp heat capacity anomalies in the PCM metallicity domain. The FST controls the kinetic factor (atomic mobility) of nucleation and growth of crystals. In the fragile state, a high kinetic factor facilitates crystallization (fast switching) at an elevated temperature by a ‘set’ pulse, while, in the strong state, a low kinetic factor hinders crystallization at ambient temperature, which is favorable for data retention. Within limits, this transition should be tunable by change of metallicity.

A recent study suggested that imminence of a M-SC/FST transition is signaled well above T_m by the combination of viscosity with diffusivity data, known as the Stokes- Einstein relation (SER)¹². In PCMs, unlike other liquids, the SER breaks down while in a high-fluidity state ($\tau \sim \text{ps}$) and even above T_m ¹².

Summary and outlook

The liquid states of PCMs are shown to be anomalous in comparison with the majority of liquid (and glassforming) chalcogenides. This appears to be due to the existence of M-SC transitions, hidden below T_m , which are driven by structure-related thermodynamic and kinetic anomalies. The knowledge of the transition-related property changes is essential for understanding of switching behaviors. The M-SC for a wide range of compositions seems to be confined to a narrow range of values of a new parameter, the metallicity M_P . Given that all PCMs are concentrated in a zone of $M_P = 0.48-0.49$, the metallicity concept may provide useful guidance for PCM designs.

Acknowledgments

PL acknowledge financial support from NSF-DMR under grant#: 1832817

References

- ¹ B.J. Eggleton, B. Luther-Davies, and K. Richardson, *Nat. Photonics* **5**, 141 (2011).
- ² Y.S. Tverjanovich, V.M. Ushakov, and A. Tverjanovich, *J Non-Cryst Solids* **197**, 235 (1996).
- ³ S.R. Ovshinsky, *Phys Rev Lett* **21**, (1968).
- ⁴ N. Yamada, E. Ohno, N. Akahira, K. Nishiuchi, K. Nagata, and M. Takao, *Jpn. J. Appl. Phys.* **26**, 61 (1987).
- ⁵ N. Yamada, E. Ohno, K. Nishiuchi, N. Akahira, and M. Takao, *J. Appl. Phys.* **69**, 2849 (1991).
- ⁶ M. Wuttig, *Nat. Mater.* **265** (2005).
- ⁷ M. Wuttig and N. Yamada, *Nat Mater* **6**, 824 (2007).
- ⁸ J. Orava, L. Greer, B. Gholipour, D.W. Hewak, and C.E. Smith, *Nat. Mater.* **11**, 279 (2012).
- ⁹ D. Loke, J.M. Skelton, W.-J. Wang, T.-H. Lee, R. Zhao, T.-C. Chong, and S.R. Elliott, *Proc. Natl. Acad. Sci.* **111**, 13272 (2014).
- ¹⁰ S. Wei, P. Lucas, and C.A. Angell, *J. Appl. Phys.* **118**, 034903 (2015).
- ¹¹ S. Wei, G.J. Coleman, P. Lucas, and C.A. Angell, *Phys. Rev. Appl.* **7**, 034035 (2017).
- ¹² S. Wei, Z. Evenson, M. Stolpe, P. Lucas, and C.A. Angell, *Sci. Adv.* **4**, eaat8632 (2018).
- ¹³ S. Bordas, M.T. Clavaguer-Mora, B. Legendre, and C. Hancheng, *Thermochim. Acta* **107**, 239 (1986).
- ¹⁴ H.S.P. Wong, S. Raoux, S. Kim, J. Liang, J.P. Reifenberg, B. Rajendran, M. Asheghi, and K.E. Goodson, *Proc. IEEE* **98**, 2201 (2010).
- ¹⁵ M. Wuttig, V.L. Deringer, X. Gonze, C. Bichara, and J.-Y. Raty, *Adv. Mater.* **0**, 1803777 (2018).
- ¹⁶ W. Zhang, R. Mazzarello, M. Wuttig, and E. Ma, *Nat. Rev. Mater.* **4**, 150 (2019).
- ¹⁷ H. Thurn and J. Ruska, *Z. Für Anorg. Allg. Chem.* **426**, 237 (1976).
- ¹⁸ S. Hosokawa, S. Yamada, and K. Tamura, *J. Non-Cryst. Solids* **156**, 708 (1993).
- ¹⁹ S. Sastry and C.A. Angell, *Nat. Mater.* **2**, 739 (2003).
- ²⁰ C. Otxacques, J.-Y. Raty, J.-P. Gaspard, Y. Tsuchiya, and C. Bichara, in *Collect. SFN* (EDP Sciences, 2011), pp. 233–245.
- ²¹ S. Hosokawa, Y. Sakaguchi, and K. Tamura, *J. Non-Cryst. Solids* **150**, 35 (1992).
- ²² Y. Tsuchiya, *J. Phys. Condens. Matter* **3**, 3163 (1991).
- ²³ C. Steimer, V. Coulet, W. Welnic, H. Dieker, R. Detemple, C. Bichara, B. Beuneu, J.-P. Gaspard, and M. Wuttig, *Adv. Mater.* **20**, 4535 (2008).
- ²⁴ W.K. Njoroge, H.-W. Wöltgens, and M. Wuttig, *J. Vac. Sci. Technol. A* **20**, 230 (2002).

²⁵ K.L. Chopra and S.K. Bahl, *J. Appl. Phys.* **40**, 4171 (1969).

²⁶ R.K. Quinn, *Mater. Res. Bull.* **9**, 803 (1974).

²⁷ F. Betts, A. Bienenstock, D.T. Keating, and J.P. deNeufville, *J. Non-Cryst. Solids* **7**, 417 (1972).

²⁸ Alekseev, Andreev, and Sadovskii, *Sov Phys Usp* **23**, 551 (1980).

²⁹ S. Hosokawa, Y. Sakaguchi, H. Hiasa, and K. Tamura, *J. Phys. Condens. Matter* **3**, 6673 (1991).

³⁰ P. Nagels, M. Rotti, and S. Vikhrov, *J. Phys. Colloq.* **42**, C4 (1981).

³¹ F. Kakinuma and S. Ohno, *J Phys Soc Jpn.* **56**, 619 (1987).

³² A.L. Allred, *J. Inorg. Nucl. Chem.* **17**, 215 (1961).

³³ P. Zalden, F. Quirin, M. Schumacher, J. Siegel, S. Wei, et al., *Science* (In press), article ID: aaw1773 (2019).

³⁴ M. Zhu, O. Cojocaru-Mirédin, A.M. Mio, J. Keutgen, M. Küpers, Y. Yu, J.-Y. Cho, R. Dronskowski, and M. Wuttig, *Adv. Mater.* **30**, 1706735 (2018).

³⁵ N. Han, S.I. Kim, J.-D. Yang, K. Lee, H. Sohn, H.-M. So, C.W. Ahn, and K.-H. Yoo, *Adv. Mater.* **23**, 1871 (2011).

³⁶ T.-Y. Lee, C. Kim, Y. Kang, D.-S. Suh, K.H.P. Kim, and Y. Khang, *Appl. Phys. Lett.* **92**, 101908 (2008).

³⁷ F. Kakinuma, S. Ohno, and K. Suzuki, *J. Non-Cryst. Solids* **117**, 575 (1990).

³⁸ H. Krebs and J. Ruska, *J. Non-Cryst. Solids* **16**, 329 (1974).

³⁹ M.H. Bhat, V. Molinero, E. Soignard, V.C. Solomon, S. Sastry, J.L. Yarger, and C.A. Angell, *Nature* **448**, 787 (2007).

⁴⁰ G. Adam and J.H. Gibbs, *J. Chem. Phys.* **43**, 139 (1965).

⁴¹ S. Wei, M. Stolpe, O. Gross, W. Hembree, S. Hechler, J. Bednarcik, R. Busch, and P. Lucas, *Acta Mater.* **129**, 259 (2017).

⁴² J. Orava, H. Weber, I. Kaban, and A.L. Greer, *J. Chem. Phys.* **144**, 194503 (2016).

⁴³ J. Orava, D.W. Hewak, and A.L. Greer, *Adv. Funct. Mater.* **25**, 4851 (2015).

⁴⁴ P. Zalden, A. von Hoegen, P. Landreman, M. Wuttig, and A.M. Lindenberg, *Chem. Mater.* **27**, 5641 (2015).

⁴⁵ M. Salinga, E. Carria, A. Kaldenbach, M. Bornhöfft, J. Benke, J. Mayer, and M. Wuttig, *Nat. Commun.* **4**, 2371 (2013).

⁴⁶ W. Zhang, I. Ronneberger, P. Zalden, M. Xu, M. Salinga, M. Wuttig, and R. Mazzarello, *Sci. Rep.* **4**, 6529 (2014).

⁴⁷ H. Flores-Ruiz and M. Micoulaut, *J. Chem. Phys.* **148**, 034502 (2018).

⁴⁸ H. Weber, J. Orava, I. Kaban, J. Pries, and A.L. Greer, *Phys. Rev. Mater.* **2**, 093405 (2018).

⁴⁹ W. Götze, *J. Phys. Condens. Matter* **11**, A1 (1999).

⁵⁰ C. A. Angell, K.L. Ngai, G.B. McKenna, P.F. McMillan, and S.W. Martin, *J. Appl. Phys.* **88**, 3113 (2000).

⁵¹ M. Schumacher, H. Weber, P. Jóvári, Y. Tsuchiya, T.G. Youngs, I. Kaban, and Riccardo Mazzarello, *Sci. Rep.* **6**, 27434 (2016).

⁵² J.A. Kalb, M. Wuttig, and F. Spaepen, *J. Mater. Res.* **22**, 748 (2007).

⁵³ F. Herwig and M. Wobst, *Z. Für Met.* **83**, 35 (1992).

⁵⁴ H. Neumann, F. Herwig, and W. Hoyer, *J. Non-Cryst. Solids* **205–207, Part 1**, 438 (1996).

⁵⁵ A. Tverjanovich, *J. Non-Cryst. Solids* **298**, 226 (2002).

⁵⁶ A. S. Tverjanovich, *Glass Phys. Chem.* **29**, 532 (2003).

⁵⁷ C.A. Angell, *Science* **267**, 1924 (1995).

⁵⁸ S.N. Yannopoulos, G.N. Papatheodorou, and G. Fytas, *Phys. Rev. B* **60**, 15131 (1999).

⁵⁹ W.-K. Rhim and K. Ohsaka, *J. Cryst. Growth* **208**, 313 (2000).

Author biographies



Shuai Wei is a postdoctoral researcher at RWTH Aachen University. He received his PhD degree in Materials Science in 2014 from Saarland University in Germany. Then he moved to the US as a Humboldt Feodor-Lynen Fellow at Arizona State University and University of Arizona before he returned to Germany joining the RWTH. His research focuses on thermodynamics, kinetics and structures of phase-change materials and amorphous metals. He received numerous awards, including RWTH Start-Up-fund, Humboldt Feodor-Lynen Fellowship, Dr.-Eduard-Martin Award, MRS Graduate Student Silver Award, and Kühborth Award. (Email: swei@physik.rwth-aachen.de).



Pierre Lucas is a professor of Materials Science & Engineering and professor of Optical Science at the University of Arizona. He received the Ph.D. in physical chemistry from Arizona State University, in 1999. Prof. Lucas has authored over 100 peer-reviewed articles and book chapters in the field of materials, calorimetry and optics. He was past chair of the Glass and Optical Materials Division of the American Ceramic Society and is a senior member of SPIE. (Contact: Materials Science & Engineering Department, University of Arizona, Email, Pierre@u.arizona.edu; Phone (520) 322 2311)



Austen Angell is a Regents' Professor at Arizona State University (ASU). He holds B.Sc. and M.Sc. degrees from Uni-Melbourne, Australia, and Ph.D. degree from Imperial College London (1961-Armstrong medal). Postdoc at Argonne Nat-Lab, then Purdue University 1966, full professor in 1971. In 1989 moved to ASU. Research interests mainly in supercooled liquids and glasses, particularly water and ionic liquids, anomalous liquids and batteries. Author of 540 papers and reviews, H-index 112 (Google scholar). Awards from ACERS (1991, Morey), ACS (2004, Hildebrand), MRS (2006, Turnbull) ECS (2010, Bredig).

